

Model C critical dynamics of random anisotropy magnets

M. Dudka^{1,2}, R. Folk², Yu. Holovatch^{1,2} and G. Moser³

¹ Institute for Condensed Matter Physics, National Acad. Sci. of Ukraine, UA-79011 Lviv, Ukraine

² Institut für Theoretische Physik, Johannes Kepler Universität Linz, A-4040 Linz, Austria

³ Institut für Physik und Biophysik, Universität Salzburg, A-5020 Salzburg, Austria

Abstract. We study the relaxational critical dynamics of the three-dimensional random anisotropy magnets with the non-conserved n -component order parameter coupled to a conserved scalar density. In the random anisotropy magnets the structural disorder is present in a form of local quenched anisotropy axes of random orientation. When the anisotropy axes are randomly distributed along the edges of the n -dimensional hypercube, *asymptotical* dynamical critical properties coincide with those of the random-site Ising model. However structural disorder gives rise to considerable effects for non-asymptotic critical dynamics. We investigate this phenomenon by a field-theoretical renormalization group analysis in the two-loop order. We study critical slowing down and obtain quantitative estimates for the effective and asymptotic critical exponents of the order parameter and scalar density. The results predict complex scenarios for the effective critical exponent approaching an asymptotic regime.

PACS numbers: 05.50.+q, 05.70.Jk, 61.43.-j, 64.60.Ak, 64.60.Ht

E-mail: maxdudka@icmp.lviv.ua, hol@icmp.lviv.ua, folk@tphys.uni-linz.ac.at

1. Introduction

In this paper, we address the peculiarities of criticality under an influence of the random anisotropy of structure. To be more specific, given a reference system is a 3d magnet with n -component order parameter which below the second order phase transition point T_c characterizes a ferromagnetic state, what will be the impact of random anisotropy [1–3] on the *critical dynamics* [4,5] of this transition? It appears, that contrary to the general believe that even weak random anisotropy destroys ferromagnetic long-range order at $d = 3$, this is true only for the isotropic random axis distribution [6]. Therefore, we will study a particular case, when the second order phase transition survives and, moreover, it remains in the random-Ising universality class [7, 8] for *any* n . A particular feature of 3d systems which belong to the random-Ising universality class is that their heat capacity does not diverge at T_c (it is the isothermal magnetic susceptibility which manifests singularity) [9]. Again, general arguments state [10, 11] that for such systems the relaxational critical dynamics of the non-conserved order parameter coupled to a conserved density, model C dynamics, degenerates to purely relaxation model without any couplings to conserved densities (model A). Nevertheless, this statement is true only in the asymptotics [12, 13] (i.e. at T_c , which in fact is never reached in experiments or in simulations). As we will show in the paper, common influence of two different factors: randomness of structure and coupling of dynamical modes leads to a rich effective critical behavior which possesses many new unexpected features.

Dynamical properties of a system near the critical point are determined by the behavior of its slow densities. In addition to the order parameter density φ these are the conserved densities. Here, we consider the case of one conserved density m . For the description of critical dynamics the characteristic time scales for the order parameter, t_φ , and for the conserved density, t_m , are introduced. Approaching the critical point, where the correlation length ξ is infinite, they are growing accordingly to the scaling laws

$$t_\varphi \sim \xi^z, \tag{1}$$

$$t_m \sim \xi^{z_m}. \tag{2}$$

These power laws define the dynamical critical exponents of the order parameter, z , and of the conserved densities, z_m . The conserved density dynamical exponents may be different from that of the order parameter.

The simplest dynamical model taking into account conserved densities is model C, [4, 14] which contains a static coupling between non-conserved n -dimensional order parameter φ and scalar conserved density m . Being quite simple, the model can be applied to the description of different physical systems. In particular, in a lattice model of intermetallic alloys [15] the non-conserved order parameter corresponds to differences in the concentration of atoms of certain kind between the odd and even sublattices. It is coupled to a conserved quantity – the concentration of atoms of this kind in the full system. In the supercooled liquids the fraction of locally favored

structures is non-conserved “bond order parameter”, coupled to the conserved density of a liquid [17]. Systems containing annealed impurities with long relaxational times [18] manifest certain similarity with the model C as well.

Dynamical properties of a model with coupling to a conserved density were less studied numerically than those for model without any coupling to secondary densities. It may be the consequence of the complexity of the numerical algorithms, which turn out to be much slower than for the simpler model. Simulations were performed for an Ising antiferromagnet with conserved full magnetization and non-conserved staggered magnetization (i.e. the order parameter) [19] and also for an Ising magnet with conserved energy [20].

Theoretical analysis of model C critical dynamics were performed by means of the field-theoretical renormalization group. Critical dynamical behavior of model C in different regions of $d - n$ plane was analyzed by $\varepsilon = 4 - d$ expansion in first order in ε [14]. The results lead to speculations about the existence of an anomalous region for $2 < n < 4$, where the order parameter is much faster than the conserved density and dynamic scaling is questionable. Recent two-loop calculation [21,22] corrected the results of Ref. [23] and showed an absence of the anomalous region $2 < n < 4$.

For the 3d model C with order parameter dimension $n = 1$, the conserved density lead to the “strong” scaling: [21,22] the dynamical exponents z and z_m coincide and are equal $2 + \alpha/\nu$, where α and ν are the specific heat and the correlation length critical exponents, correspondingly. For the Ising system ($n = 1$) the specific heat diverges and $\alpha > 0$. While for a system with $\alpha < 0$, that is for the physically interesting cases $n = 2, 3$, the scalar density decouples from the order parameter density in the asymptotic region. It means that for such values of n the order parameter scales with the same dynamical critical exponent z as in the model A and the dynamical exponent of the scalar density is equal to $z_m = 2$. The importance of the sign of α was already mentioned in Ref. [14].

A rich critical dynamical behavior has already been observed in system with structural disorder [18,24–27]. Interest in this case is increased by the fact that real materials are always characterized by some imperfection of their structure. Obviously, that models describing their properties should contain terms connected with structural disorder of certain type. For the static behavior of a system with quenched energy coupled disorder (e.g. dilution), the Harris criterion [28] states that disorder does not lead to a new static universality class if the heat capacity of the pure system does not diverge, that is $\alpha < 0$. It appears that in diluted systems $\alpha < 0$ is always the case (see Ref. [9]). The conclusion about influence of coupling between order parameter and secondary density works also in this case. The presence of a secondary density does not affect the dynamical critical properties in the asymptotics [10]: order parameter dynamics is the same as in an appropriate model A, and $z_m = 2$. Nevertheless, as we noted at the beginning, the coupling between the order parameter and the secondary density considerably influences the non-asymptotic critical behavior [12,13].

We are interested in the critical dynamics of a systems with structural disorder of

another type, namely, random anisotropy magnets. Their properties are described by the random anisotropy model (RAM) introduced in Ref. [1]. In this spin lattice model each spin is subjected to a local anisotropy of random orientation, which essentially is described by a vector and therefore is defined only for $n > 1$. The Hamiltonian reads: [1]

$$\mathcal{H} = - \sum_{\mathbf{R}, \mathbf{R}'} J_{\mathbf{R}, \mathbf{R}'} \vec{S}_{\mathbf{R}} \vec{S}_{\mathbf{R}'} - \bar{D} \sum_{\mathbf{R}} (\hat{x}_{\mathbf{R}} \vec{S}_{\mathbf{R}})^2, \quad (3)$$

where, $\vec{S} = (S^1, \dots, S^n)$, are n -component vectors located on the sites \mathbf{R} of a d -dimensional cubic lattice, $\bar{D} > 0$ is an anisotropy constant, \hat{x} is a random unit vector pointing in direction of the local anisotropy axis. The short-range interaction $J_{\mathbf{R}, \mathbf{R}'}$ is assumed to be ferromagnetic.

The static critical behavior of RAM was analyzed by many theoretical and numerical investigations which could be compared with the critical properties of random anisotropy magnets found in experiments (for recent review see Ref. [3]). The results of this analysis bring about that random anisotropy magnets do not show a second order phase transition for an isotropic random axis distribution. However they possibly undergo a second-order phase transition for an anisotropic distribution (for references see reviews Refs. [2,3]). Renormalization group studies of the asymptotic [7,8,29–31] and non-asymptotic properties [3] of RAM corroborated such a conclusion. For example, the RAM with random axes distributed due to the so-called cubic distribution was shown within two-loop approximation to undergo a second order phase transition governed by the random Ising critical exponents, [3, 8] as first suggested in Ref. [7]. Recently this result found its confirmation in a five-loop RG study [31]. The cubic distribution allows \hat{x} to point only along one of the $2n$ directions of the axes \hat{k}_i of a (hyper)cubic lattice: [29]

$$p(\hat{x}) = \frac{1}{2n} \sum_{i=1}^n \left[\delta^{(n)}(\hat{x} - \hat{k}_i) + \delta^{(n)}(\hat{x} + \hat{k}_i) \right], \quad (4)$$

where $\delta(y)$ are Kronecker's deltas.

Contrary to the static critical behavior of random anisotropy magnets their dynamics was less investigated. Only dynamical models for systems with isotropic distribution were briefly discussed in Refs. [32,33]. The critical dynamics was discussed within model A, Ref. [34], and the dynamical exponents were calculated. However, it does not give a comprehensive quantitative description since it is (i) restricted to the isotropic distribution of the random axis and (ii) it is performed only within the first non-trivial order of $\varepsilon = 4 - d$ expansion.

The model A critical dynamics of RAM with cubic random axis distribution was analyzed within two-loop approximation in Ref. [35] Although the asymptotic dynamical properties found coincide with those of the random-site Ising model, the non-asymptotic behavior is strongly influenced by the presence of random anisotropy [35].

Beside the slow order parameter an additional slow conserved densities might be present, for instance the energy density. Therefore considering the non-asymptotic dynamical behavior of the RAM an extension to model C is of interest. Indeed, there

exist magnets where the distribution of the local random axes is anisotropic (e.g. the rare earth compounds, see Ref. [3]).

The structure of the paper is as follows: Section 2 presents the equations defining the dynamical model and its Lagrangian, the renormalization is performed in Section 3, there the asymptotic and effective dynamical critical exponents are defined. In Section 4 we give the expressions for the field-theoretic functions in two-loop order and the resulting non-asymptotic behavior is discussed. Section 5 summarizes our study. Details of the perturbation expansion are presented in the appendix.

2. Model equations

Here we consider the dynamical model for random anisotropy systems described by (3) with random axis distribution (4). The structure of the equations of motion for n -component order parameter $\vec{\varphi}_0$ and secondary density [4, 14] m_0 is not changed by presence of random anisotropy

$$\frac{\partial \varphi_{i,0}}{\partial t} = -\overset{\circ}{\Gamma} \frac{\partial \mathcal{H}}{\partial \varphi_{i,0}} + \theta_{\varphi_i}, \quad i = 1 \dots n, \quad (5)$$

$$\frac{\partial m_0}{\partial t} = \overset{\circ}{\lambda} \nabla^2 \frac{\partial \mathcal{H}}{\partial m_0} + \theta_m. \quad (6)$$

The order parameter relaxes and conserved density diffuses with the kinetic coefficients $\overset{\circ}{\Gamma}$, $\overset{\circ}{\lambda}$ correspondingly. The stochastic forces θ_{φ_i} , θ_m obey the Einstein relations:

$$\langle \theta_{\varphi_i}(x, t) \theta_{\varphi_j}(x', t') \rangle = 2\overset{\circ}{\Gamma} \delta(x - x') \delta(t - t') \delta_{ij}, \quad (7)$$

$$\langle \theta_m(x, t) \theta_m(x', t') \rangle = -2\overset{\circ}{\lambda} \nabla^2 \delta(x - x') \delta(t - t') \delta_{ij}. \quad (8)$$

The disorder-dependent equilibrium effective static functional \mathcal{H} describing behavior of system in the equilibrium reads:

$$\mathcal{H} = \int d\mathbf{R} \left\{ \frac{1}{2} \left[|\nabla \vec{\varphi}_0|^2 + \overset{\circ}{r} |\vec{\varphi}_0|^2 \right] + \frac{\overset{\circ}{v}}{4!} |\vec{\varphi}_0|^4 - D_0 (\hat{x} \vec{\varphi}_0)^2 + \frac{1}{2} m_0^2 + \frac{1}{2} \overset{\circ}{\gamma} m_0 |\vec{\varphi}_0|^2 - \overset{\circ}{h} m_0 \right\}, \quad (9)$$

where D_0 is an anisotropy constant proportional to \bar{D} of Eq. (3), $\overset{\circ}{r}$ and $\overset{\circ}{v}$ depend on \bar{D} and the coupling of the usual ϕ^4 model.

Integrating out the secondary density one reduces (9) to usual Ginzburg-Landau-Wilson model with random anisotropy term and new parameter $\overset{\circ}{v}$ and $\overset{\circ}{r}$ connected to the model parameters $\overset{\circ}{r}$, $\overset{\circ}{v}$, $\overset{\circ}{\gamma}$ and h via relations:

$$\overset{\circ}{r} = \overset{\circ}{r} + \overset{\circ}{\gamma} \overset{\circ}{h}, \quad \overset{\circ}{v} = \overset{\circ}{v} - 3\overset{\circ}{\gamma}^2 \quad (10)$$

We study the critical dynamics by applying the Bausch-Janssen-Wagner approach [36] of dynamical field-theoretical renormalization group (RG). In this approach, the critical behavior is studied on the basis of long-distance and long-time properties of the Lagrangian incorporating features of dynamical equations of the model. The model defined by expressions (5)-(9) within Bausch-Janssen-Wagner formulation [36] turns out

to be described by an unrenormalized Lagrangian:

$$\begin{aligned} \mathcal{L} = \int d\mathbf{R}dt \left\{ -\dot{\Gamma} \sum_{i=1}^n \tilde{\varphi}_{0,i} \tilde{\varphi}_{0,i} + \sum_{i=1}^n \tilde{\varphi}_{0,i} \left(\frac{\partial}{\partial t} + \dot{\Gamma}(\dot{\mu} - \nabla^2) \right) \varphi_{0,i} + \right. \\ \left. \dot{\lambda} \tilde{m}_0 \nabla^2 \tilde{m}_0 + \tilde{m}_0 \left(\frac{\partial}{\partial t} - \dot{\lambda} \nabla^2 \right) m_0 + \sum_i \frac{1}{3!} \dot{\Gamma} \dot{v} \tilde{\varphi}_{0,i} \varphi_{0,i} \sum_j \varphi_{0,j} \varphi_{0,j} + \right. \\ \left. \sum_j 2\dot{\Gamma} D_0(\hat{x} \tilde{\varphi}_{0,i}(t))(\hat{x} \varphi_{0,i}(t)) + \dot{\Gamma} \dot{\gamma} m_0 \tilde{\varphi}_{0,i} \varphi_{0,i} - \frac{1}{2} \dot{\lambda} \dot{\gamma} \tilde{m}_0 \nabla^2 \varphi_{0,i} \varphi_{0,i} \right\}, \quad (11) \end{aligned}$$

with auxiliary response fields $\tilde{\varphi}_i(t)$. There are two ways to average over the disorder configurations for dynamics. The first way originates from statics and consists in using the replica trick, [37] where N replicas of the system are introduced in order to facilitate configurational averaging of the corresponding generating functional. Finally the limit $N \rightarrow 0$ has to be taken.

However we follow the second way proposed in Ref. [33]. There it was shown that the replica trick is not necessary if one takes just the average of the Lagrangian with respect to the distribution of random variables. The Lagrangian obtained in this way is described by the following expression:

$$\begin{aligned} \mathcal{L} = \left\{ \int d\mathbf{R}dt \sum_i \tilde{\varphi}_{i,0} \left[\left(\frac{\partial}{\partial t} + \dot{\Gamma}(\dot{\mu} - \nabla^2) \right) \varphi_{i,0} - \dot{\Gamma} \tilde{\varphi}_i + \frac{\dot{\Gamma} \dot{v}}{3!} \varphi_{i,0} \sum_j \varphi_{j,0} \varphi_{j,0} + \right. \right. \\ \left. \frac{\dot{\Gamma} \dot{y}}{3!} \varphi_{i,0}^3 \right] + \dot{\lambda} \tilde{m}_0 \nabla^2 \tilde{m}_0 + \tilde{m}_0 \left(\frac{\partial}{\partial t} - \dot{\lambda} \nabla^2 \right) m_0 + \dot{\Gamma} \dot{\gamma} m_0 \tilde{\varphi}_{i,0} \varphi_{i,0} - \\ \frac{1}{2} \dot{\lambda} \dot{\gamma} \tilde{m}_0 \nabla^2 \varphi_{i,0} \varphi_{i,0} + \int dt' \sum_i \tilde{\varphi}_{i,0}(t) \varphi_{i,0}(t) \left[\frac{\dot{\Gamma}^2 \dot{u}}{3!} \sum_j \tilde{\varphi}_{j,0}(t') \varphi_{j,0}(t') + \right. \\ \left. \frac{\dot{\Gamma}^2 \dot{w}}{3!} \tilde{\varphi}_{i,0}(t') \varphi_{i,0}(t') \right] \left. \right\}. \quad (12) \end{aligned}$$

In Eq. (12), the bare mass is $\dot{\mu} = \dot{r} - D/n$, and bare couplings are $\dot{u} > 0$, $\dot{v} > 0$, $\dot{w} < 0$. Terms with couplings \dot{u} and \dot{w} are generated by averaging over configurations and the values of \dot{u} and \dot{w} are connected to the moments of distribution (4). Therefore the ratio of the two couplings has to be $\dot{w}/\dot{u} = -n$. The \dot{y} -term in (12) does not result from the averaging procedure but has to be included since it is generated in the perturbational treatment. It can be of either sign.

3. RG functions

We perform renormalization within minimal subtraction scheme introducing renormalization factors Z_{a_i} , $a_i = \{\{\alpha\}, \{\delta\}\}$, leading to the renormalized parameters $\{\alpha\} = \{u, v, w, y, \gamma, \Gamma, \lambda\}$ and renormalized densities $\{\delta\} = \{\varphi, \tilde{\varphi}, m, \tilde{m}\}$. For the specific heat we need also an additive renormalization A_{φ^2} which leads to the function

$$B_{\varphi^2}(u, \Delta) = \mu^\varepsilon Z_{\varphi^2}^2 \mu \frac{d}{d\mu} \left(Z_{\varphi^2}^{-2} \mu^{-\varepsilon} A_{\varphi^2} \right), \quad (13)$$

with the scale parameter μ and factor Z_{φ^2} that renormalizes the vertex with φ^2 insertion. From the Z -factors one obtains the ζ -functions describing the critical properties

$$\zeta_a(\{\alpha\}) = -\frac{d \ln Z_a}{d \ln \mu}, \quad (14)$$

Relations between the renormalization factors lead to corresponding relations between the ζ -functions. In consequence for the description of the critical dynamics one needs only ζ -functions of the couplings, ζ_{u_i} ($u_i = \{u, v, w, y\}$ for $i = 1, 2, 3, 4$), the order parameter ζ_φ , the auxiliary field $\zeta_{\bar{\varphi}}$, φ^2 -insertion ζ_{φ^2} and also function B_{φ^2} . In particular, the ζ -function of the time scale ratio

$$W = \frac{\Gamma}{\lambda} \quad (15)$$

introduced for the description of dynamic properties is related to the above ζ -functions:

$$\zeta_W = \frac{1}{2}\zeta_\varphi - \frac{1}{2}\zeta_{\bar{\varphi}} - \gamma^2 B_{\varphi^2}. \quad (16)$$

The behavior of the model parameters under renormalization is described by the flow equations

$$\ell \frac{d\{\alpha\}}{d\ell} = \beta_{\{\alpha\}}. \quad (17)$$

The β -functions for the static model parameters have the following explicit form:

$$\beta_{u_i} = u_i(\varepsilon + \zeta_\varphi + \zeta_{u_i}), \quad (18)$$

$$\beta_\gamma = \gamma\left(\frac{\varepsilon}{2} + \zeta_{\varphi^2} + \frac{\gamma^2}{2} B_{\varphi^2}\right). \quad (19)$$

The dynamic β -function for the time scale ratio W reads

$$\beta_W = W\zeta_W = W\left(\frac{1}{2}\zeta_\varphi - \frac{1}{2}\zeta_{\bar{\varphi}} - \gamma^2 B_{\varphi^2}\right). \quad (20)$$

The asymptotic critical behavior of the system is obtained from the knowledge of the fixed points (FPs) of the flow equations (17). A FP $\{\alpha^*\} = \{u^*, v^*, w^*, y^*, \gamma^*, W^*\}$ is defined as simultaneous zero of the β -functions. The set of equations for the static fourth order couplings decouple from the other β -functions. Thus for each of the FPs of the static fourth order couplings $\{u_i^*\}$ one obtains two FP values of the static coupling between the order parameter and the conserved density γ :

$$\gamma^{*2}=0 \quad \text{and} \quad \gamma^{*2} = \frac{\varepsilon - 2\zeta_{\varphi^2}(\{u_i^*\})}{B_{\varphi^2}(\{u_i^*\})} = \frac{\alpha}{\nu B_{\varphi^2}(\{u_i^*\})}, \quad (21)$$

where α and ν are the heat capacity and correlation length critical exponent calculated at the corresponding FP $\{u^*\}$. Inserting the obtained values for the static FPs into the β -function (20) one finds the corresponding FP values of the time scale ratio W .

The stable FP accessible from the initial conditions corresponds to the critical point of system. A FP is stable if all eigenvalues ω_i of the stability matrix $\partial\beta_{\alpha_i}/\partial\alpha_j$ calculated at this FP have positive real parts. The values of ω_i indicate also how fast the renormalized model parameters reach their fixed point values.

From the structure of β -functions we conclude, that the stability of any FP with respect to the parameters γ and W is determined solely by the derivatives of the corresponding β -functions:

$$\omega_\gamma = \frac{\partial\beta_\gamma}{\partial\gamma}, \quad \omega_W = \frac{\partial\beta_W}{\partial W}. \quad (22)$$

Moreover using (19) we can write:

$$\omega_\gamma = -\frac{\varepsilon - 2\zeta_{\varphi^2}(\{u_i\})}{2} + \frac{3}{2}\gamma^2 B_{\varphi^2}(u, \Delta), \quad (23)$$

which at the FP $\{\alpha^*\}$ leads to:

$$\omega_\gamma|_{\{\alpha\}=\{\alpha^*\}} = -\frac{\alpha}{2\nu} \quad \text{for} \quad \gamma^{*2} = 0, \quad (24)$$

$$\omega_\gamma|_{\{\alpha\}=\{\alpha^*\}} = \frac{\alpha}{\nu} \quad \text{for} \quad \gamma^{*2} \neq 0. \quad (25)$$

Therefore, a stability with respect to parameter γ is determined by the sign of the specific heat exponent α . For a system with non-diverging heat capacity ($\alpha < 0$) at the critical point, $\gamma^* = 0$ is the stable FP. Static results report that the stable and accessible FP is of a random site Ising type. In this case $\alpha < 0$. This leads to the conclusions that in the asymptotic region the secondary density decouples from the order parameter.

The critical exponents are defined by the FP values of the ζ -functions. For instance, the asymptotic dynamical critical exponent z is expressed at the stable FP by:

$$z = 2 + \zeta_\Gamma(\{\alpha^*\}), \quad (26)$$

with

$$\zeta_\Gamma(\{\alpha\}) = \frac{1}{2}\zeta_\varphi(\{u_i\}) - \frac{1}{2}\zeta_{\bar{\varphi}}(\{\alpha\}). \quad (27)$$

In similar way the dynamical critical exponent z_m for the secondary density is defined by:

$$z_m = 2 + \zeta_m(\{u_i^*\}, \gamma^*), \quad (28)$$

where

$$\zeta_m(\{u_i\}, \gamma) = \frac{1}{2}\gamma^2 B_{\varphi^2}(\{u_i\}). \quad (29)$$

While their effective counterparts in the non asymptotic region are defined by the solution of flow equations (17) as

$$z^{\text{eff}} = 2 + \zeta_\Gamma(\{u_i(\ell)\}, \gamma(\ell), W(\ell)), \quad (30)$$

$$z_m^{\text{eff}} = 2 + \zeta_m(\{u_i(\ell)\}, \gamma^2(\ell)). \quad (31)$$

In the limit $\ell \rightarrow 0$ the effective exponents reach their asymptotic values. In the next section we analyze the possible scenarios of effective dynamical behavior as well as check the approach to the asymptotical regime.

4. Results

4.1. Asymptotic properties

The static two-loop RG functions of RAM with cubic random axis distribution in the minimal subtraction scheme agree with the results obtained in Ref. [3] using the replica trick and read:

$$\begin{aligned} \beta_u = & -\varepsilon u + \frac{4}{3}u^2 + \frac{n+2}{3}vu + \frac{2}{3}uw + yu + \frac{1}{3}wv - \frac{7}{6}u^3 - \frac{11(n+2)}{18}vu^2 \\ & - \frac{5(n+2)}{36}v^2u - \frac{11}{9}u^2w - \frac{5}{18}uw^2 - \frac{11}{6}u^2y - \frac{5}{12}y^2u - \\ & \frac{3}{2}vuw - \frac{5}{6}wyu - \frac{5}{6}vwy - \frac{1}{9}v^2w - \frac{1}{9}w^2v, \end{aligned} \quad (32)$$

$$\begin{aligned} \beta_v = & -\varepsilon v + \frac{n+8}{6}v^2 + 2vu + \frac{2}{3}wv + yv - \frac{3n+14}{12}v^3 - \frac{11n+58}{18}v^2u - \frac{41}{18}vu^2 - \\ & \frac{5}{18}w^2v - \frac{5}{6}vwy - \frac{31}{18}v^2w - \frac{11}{6}v^2y - \frac{5}{12}y^2v - \frac{17}{6}vuy - \frac{17}{9}wvu, \end{aligned} \quad (33)$$

$$\begin{aligned} \beta_w = & -\varepsilon w + \frac{4}{3}w^2 + 2wu + \frac{2}{3}wv + yw - \frac{7}{6}w^3 - \frac{29}{9}w^2u - \frac{41}{18}wu^2 - \frac{31}{18}w^2v - \\ & \frac{n+10}{36}v^2w - \frac{11}{6}w^2y - \frac{5}{12}y^2w - \frac{17}{6}wuy - \frac{5n+34}{18}wvu - \frac{5}{6}vwy, \end{aligned} \quad (34)$$

$$\begin{aligned} \beta_y = & -\varepsilon y + \frac{3}{2}y^2 + 2yu + 2yv + 2wy + \frac{4}{3}wv - \frac{17}{12}y^3 - \frac{41}{18}u^2y - \\ & \frac{23}{6}y^2u - \frac{23}{6}y^2v - \frac{23}{6}y^2w - \frac{5n+82}{36}v^2y - \frac{41}{18}w^2y - 2w^2v - \\ & \frac{n+18}{9}v^2w - \frac{41}{6}vwy - \frac{41}{9}wyu - \frac{5n+82}{18}vuy - \frac{8}{3}vuw, \end{aligned} \quad (35)$$

$$\zeta_\varphi = \frac{1}{36}u^2 + \frac{y^2}{24} + \frac{1}{36}w^2 + \frac{n+2}{72}v^2 + \frac{yu}{12} + \frac{wv}{12} + \frac{yv}{12} + \frac{n+2}{36}vu + \frac{wu}{18} + \frac{wy}{12}, \quad (36)$$

$$\begin{aligned} \zeta_{\varphi^2} = & \frac{1}{3}u + \frac{n+2}{6}v + \frac{1}{3}w + \frac{y}{2} - \frac{5}{12}u^2 - \frac{5}{n+2}12v^2 - \frac{5}{6}w^2 - \frac{5}{4}y^2 - \\ & \frac{5n+2}{6}vu - \frac{5}{3}wu - 5\frac{yu}{2} - 5\frac{wv}{2} - 5\frac{yv}{2} - 5\frac{wy}{2}. \end{aligned} \quad (37)$$

Here, u, v, w, y stand for the renormalized couplings.

Given the expression for the function ζ_{φ^2} , Eq. (37), the function β_γ can be constructed via Eq. (19) and the two-loop expression $B_{\varphi^2} = n/2$.

In order to discuss the dynamical FPs it turns out to be useful to introduce the parameter $\rho = W/(1+W)$ which maps W and its FPs into a finite region of the

parameter space ρ . Then instead of the flow equation for W the flow equation for ρ arises in (17):

$$\ell \frac{d\rho}{d\ell} = \beta_\rho(\{u_i\}, \gamma, \rho), \quad (38)$$

where according to (20)

$$\beta_\rho(\{u_i\}, \gamma, \rho) = \rho(\rho - 1)(\zeta_\Gamma(\{u_i\}, \gamma, \rho) - \gamma^2 B_{\varphi^2}(\{u_i\})). \quad (39)$$

The function ζ_Γ in the above expression is obtained from Eq (27) using the static function ζ_φ (36) and the two loop result for the dynamic function $\zeta_{\bar{\varphi}}$ (calculated from Eq (A.8)). We get the following two-loop expression for ζ_Γ :

$$\begin{aligned} \zeta_\Gamma = & -\frac{u+w}{3} + \gamma^2 \rho + \frac{(6 \ln(4/3) - 1)}{24} \left(\frac{(n+2)}{3} v^2 + \frac{2}{3} v y + y^2 \right) + \\ & \frac{1}{36} (5u^2 + (n+2)uv + 10uw + 3uy + 3vw + 5w^2 + 3wy) - \\ & \frac{\rho \gamma^2}{2} \left(\left(\frac{(n+2)}{3} v + y \right) (1 - 3 \ln(4/3)) + \right. \\ & \left. \rho \gamma^2 \left(\frac{n}{2} - \rho - \frac{3(n+2)}{2} \ln(4/3) + (1+\rho) \ln(1-\rho^2) \right) + u + w \right) + \\ & \gamma^2 \rho \left(\frac{u+w}{6} \right) \left(\frac{\rho^2 \ln(\rho)}{1-\rho} + (3+\rho) \ln(1-\rho) \right). \end{aligned} \quad (40)$$

The two-loop result [22] for the pure model C is recovered by setting in (40) the couplings u, w, y equal to zero. While setting $\gamma = 0$ in (40) the result for model A with random anisotropy [35] is recovered. The $\gamma^2 u, \gamma^2 w, \gamma^2 y$ -terms represent the intrinsic contribution of model C for random anisotropy magnets.

There are two different ways to proceed with the numerical analysis of the perturbative expansions for the RG functions (32) - (35), (40). The first one is an ε -expansion [38] whereas the second one is the so-called fixed-dimension approach [39]. In the frames of the latter approach, one fixed ε and solves the non-linear FP equations directly at the space dimension of interest (i.e. at $\varepsilon = 1$ in our $d = 3$ case). Whilst in many problems these two ways serve as complementing ones, it appears that for certain cases only one of them, namely the fixed- d approach leads to the quantitative description. Indeed, as it is well known by now, the ε -expansion turns into the $\sqrt{\varepsilon}$ -expansion for the random-site Ising model and no reliable numerical estimates can be obtained on its basis (see [9] and references therein). As one will see below, the random-site Ising model behavior emerges in our problem as well, therefore we proceed within the fixed- d approach.

The series for RG functions are known to diverge. Therefore to obtain reliable results on their basis we apply the Padé-Borel resummation procedure [40] to the static functions. It is performed in following way: we construct the Borel image of the resolvent series [41] of the initial RG function f :

$$f = \sum_{0 \leq i+j+l+k \leq 2} a_{i,j,k,l} (ut)^i (vt)^j (wt)^k (yt)^l \rightarrow$$

$$\sum_{0 \leq i+j+l+k \leq 2} \frac{a_{i,j,k,l} u^i v^j w^k y^l t^{i+j+k+l}}{\Gamma(i+j+1)},$$

where f stands for one of the static RG functions β_{u_i} , $\beta_\gamma/\gamma - \gamma^2 n/4$, $a_{i,j,k,l}$ are the corresponding expansion coefficients given by Eqs. (32)–(37), and $\Gamma(i+j+1)$ is Euler's gamma function. Then, the Borel image is extrapolated by a rational Padé approximant [42] $[K/L](t)$. Within two-loop approximation we use the diagonal approximant with linear denominator $[1/1]$. As it is known in the Padé analysis, the diagonal approximants ensure the best convergence of the results [42]. The resummed function is then calculated by an inverse Borel transform of this approximant:

$$f^{res} = \int_0^\infty dt \exp(-t) [1/1](t). \quad (41)$$

As far as the above procedure enables one to restore correct static RG flow (as sketched below) we do not further resum the dynamic RG function β_W .

The analysis of the static functions $\beta_{\{u_i\}}$ at fixed dimension $d = 3$ brings about an existence of 16 FPs [3, 31]. Only ten of these FPs are situated in the region of physical interest $u > 0$, $v > 0$, $w < 0$. Corresponding values of FP coordinates can be found in Ref. [3].

For each static FP $\{u_i^*\}$ we obtain a set of dynamical FPs with different γ^* and ρ^* . The FPs obtained for $n = 2, 3$ are listed in Table 1 and Table 2 correspondingly. Stability exponents ω_γ and ω_ρ are given in tables as well. Here we keep the numbering of FPs already used in Refs. [3, 8, 29, 31, 35]. It is known from the statics that FP XV governs the critical behavior of RAM with cubic distribution. This FP is of the same origin as the FP of random-site Ising model therefore all static critical exponents coincide with those of the random-site Ising model. Since the specific heat exponent in this case is negative, the asymptotic critical dynamics is described by model A. However the non-asymptotic critical properties of random anisotropy magnets are different from the random-site Ising magnets in statics [3] as well as in dynamics [35]. Moreover, for the model C considered here, the non-asymptotic critical behavior differs considerably from that of the corresponding model A as we will see below.

4.2. Non-asymptotic properties

The existence of such a large number of dynamical FPs makes non-asymptotic critical behavior more complex as in model A. We present here results for $n = 3$. For $n = 2$ the behavior is qualitatively similar. Solving the flow equations for different initial conditions we obtain different flows in the space of model parameters. The projection of most characteristic flows into the subspace $w - y - \rho$ is presented in Fig. 1. The open circles indicate genuine model C unstable FPs whereas filled circles represent model A unstable FPs. The filled square denotes the stable FP.

The initial conditions for the couplings $u(0), v(0), w(0), y(0)$ for the flows shown are the same as those in Refs. [3, 35]. We choose $\gamma(0) = 0.1$ and $\rho(0) = 0.6$. Many flows are affected by the two Ising FPs V_C and X_C . Inserting the solutions of the flow

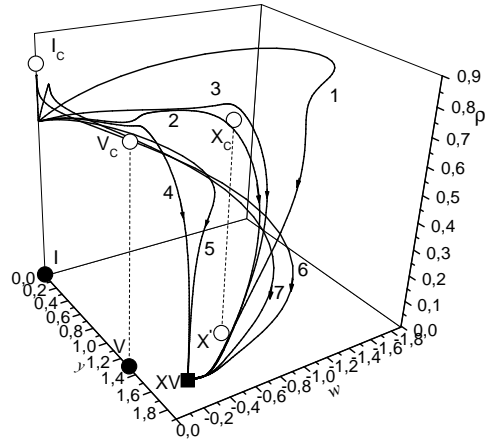


Figure 1. Projections of flows for $n = 3$ in the subspace of couplings $w - y - \rho$. Open circles represent projections of unstable FPs with non-zero γ^* . Filled circles denote unstable FPs with $\gamma^* = 0$. The filled square shows the stable FP. See Section 4.2 for a more detailed description.

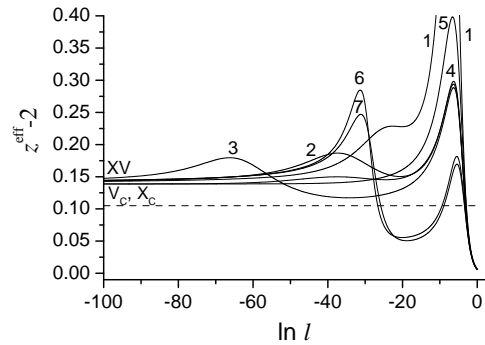


Figure 2. Dependence of the order parameter effective dynamical critical exponent in the model C dynamics on the logarithm of flow parameter. See text for full description.

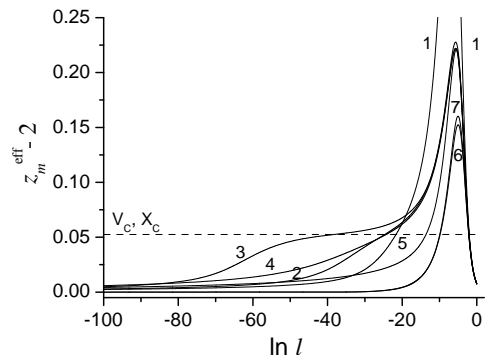


Figure 3. Dependence of the conserved density effective dynamical critical exponent in the model C dynamics on the logarithm of flow parameter. See text for full description.

Table 1. Two-loop values for the dynamical FPs of random anisotropy magnets with $n = 2$ (model C).

FP	γ^*	ρ^*	ω_γ	ω_ρ	z
I	0	$0 \leq \rho^* \leq 1$	0	0	2
I'	1	0	1	-1	2
I_C	1	0.6106	1	0.745	3
I'₁	1	1	1	$-\infty$	∞
II	0	0	0.0387	0.0526	2.0526
II₁	0	1	0.0387	-0.0526	2.0526
III	0	0	-0.1686	-0.1850	1.8150
III₁	0	1	-0.1686	0.1850	1.8150
III_C	.5806	0	0.3371	-0.5222	1.8150
III'₁	.5806	1	0.3371	∞	$-\infty$
V	0	0	-0.0525	0.0523	2.0523
V₁	0	1	-0.0525	-0.0523	2.0523
V'	.3240	0	0.1050	-0.0527	2.0523
V_C	.3240	0.5241	0.1050	0.0277	2.1050
V'₁	.3240	1	0.1050	$-\infty$	∞
VI	0	0	-0.0049	-0.0417	2.0107
VI₁	0	1	-0.0049	0.0417	2.0107
VI'	0.0986	0	0.0097	0.00095	2.0107
VI'₁	0.0986	1	0.0097	∞	$-\infty$
VIII	0	0	-0.0525	0.1569	2.1569
VIII₁	0	1	-0.0525	-0.1569	2.1569
VIII'	0.3240	0	0.1050	0.0519	2.1569
VIII'₁	0.3240	1	0.1050	$-\infty$	∞
X	0	0	-0.0525	0.0523	2.0523
X₁	0	1	-0.0525	-0.0523	2.0523
X'	.3240	0	0.1050	-0.0527	2.0523
X_C	.3240	0.5241	0.1050	0.0277	2.1050
X'₁	.3240	1	0.1050	$-\infty$	∞
XV	0	0	0.0018	0.1388	2.1388
XV₁	0	1	0.0018	-0.1388	2.1388

equations into the expressions for dynamical exponents we obtain the effective exponents z^{eff} and z_m^{eff} . The dependence of z^{eff} on the flow parameter ℓ corresponding to flows 1-7 is shown in Fig. 2. Similarly Fig 3 shows this dependence for the effective exponent of the conserved density z_m^{eff} . Flow 3 is affected by both FPs V_C and X_C . Therefore the effective exponents demonstrate a region with values which are close to those for model C in the case of the Ising magnet (see curves 3 in Figs. 2 and 3). The asymptotic values corresponding to the FPs V_C and X_C are indicated by the dashed line. They correspond

Table 2. Two-loop values for the dynamical FPs of random anisotropy magnets with $n = 3$ (model C).

FP	γ^*	ρ^*	ω_γ	ω_ρ	z
I	0	$0 \leq \rho^* \leq 1$	0	0	2
I'	0.8165	0	1	-1	2
I_C	0.8165	0.7993	1	0.5218	3
I'₁	0.8165	1	1	$-\infty$	∞
II	0	0	0.1109	0.0506	2.0506
II₁	0	1	0.1109	-0.0506	2.0506
III	0	0	-0.1686	-0.1850	1.8150
III₁	0	1	-0.1686	0.1850	1.8150
III'	0.4741	0	.3371	-0.5222	1.8150
III'₁	0.4741	1	0.3371	∞	$-\infty$
V	0	0	-0.0525	0.0523	2.0523
VI₁	0	1	-0.0525	-0.0523	2.0523
VI'	0.2646	0	0.1050	-0.0527	2.0523
VI_C	0.2646	0.7617	0.1050	0.0157	2.1050
VI'₁	0.2646	1	0.1050	$-\infty$	∞
VI	0	0	-0.0162	-0.0401	1.9599
VI₁	0	1	-0.0162	0.0401	1.9599
VI'	0.1467	0	0.0323	-0.0724	1.9599
VI'₁	0.1467	1	0.0323	∞	$-\infty$
VIII	0	0	0.1051	0.0425	2.0425
VIII₁	0	1	0.1051	-0.0425	2.0425
IX	0	0	-0.0161	-0.0384	1.9616
IX₁	0	1	-0.0161	0.0384	1.9616
IX'	0.1466	0	0.0322	-0.0707	1.9616
IX'₁	0.1466	1	0.0322	∞	$-\infty$
X	0	0	-0.0525	0.0523	2.0523
X₁	0	1	-0.0525	-0.0523	2.0523
X'	0.2646	0	0.1050	-0.0527	2.0523
X_C	0.2646	0.7617	0.1050	0.0157	2.1050
X'₁	0.2646	1	0.1050	$-\infty$	∞
XV	0	0	0.0018	0.1388	2.1388
XV₁	0	1	0.0018	-0.1388	2.1388

to the values asymptotically obtained in the pure model C with $n = 1$, since the FPs V_C and X_C are of the same origin, that FP of pure model C. Curves 6 correspond to flows near the pure FP II. Whereas curve 7 corresponds to the flow near the cubic FP VIII.

The main difference of the behavior of the effective dynamical exponent z^{eff} in model C from that in model A is the appearance of curves with several peaks. The value of the peak appearing on the right-hand side depends on the initial condition $\gamma(0)$ and $\rho(0)$. This is demonstrated in Fig.4.

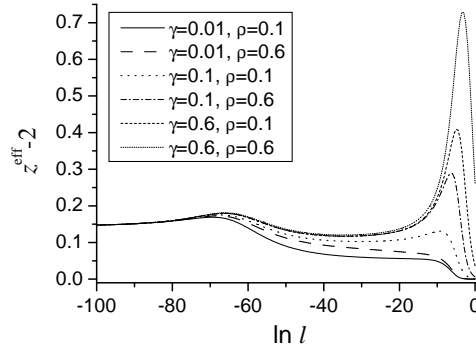


Figure 4. Dependence of z^{eff} on the logarithm of flow parameter for different initial values γ and ρ

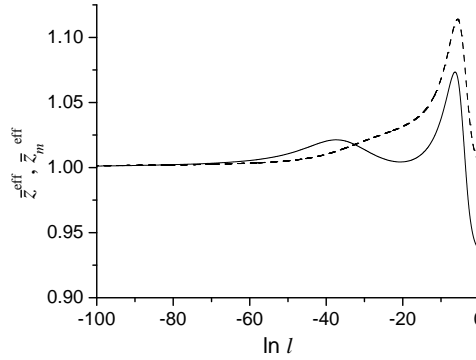


Figure 5. Normalized effective dynamical critical exponents of order parameter and conserved density \bar{z}^{eff} (solid line), \bar{z}_m^{eff} (dashed line) correspondent to flow 2.

The effective behavior of the two dynamical critical exponents for the order parameter and the conserved density might be quite different as one sees comparing Figs. 2 and 3. However, one may ask if both exponents reach the asymptotic values in the same way. For this purpose we introduce a normalization of the values of the effective exponents by their values in the asymptotics. In particular, we introduce notations $\bar{z}^{\text{eff}} = z^{\text{eff}}/z$, $\bar{z}_m^{\text{eff}} = z_m^{\text{eff}}/z_m$ for order parameter exponent and conserved density exponent correspondingly. Figs. 5, 6 show behavior of normalized exponents for order parameter and conserved density for flows 2 and 4 correspondingly. It illustrates that approach to the asymptotics for order parameter exponents and conserved density

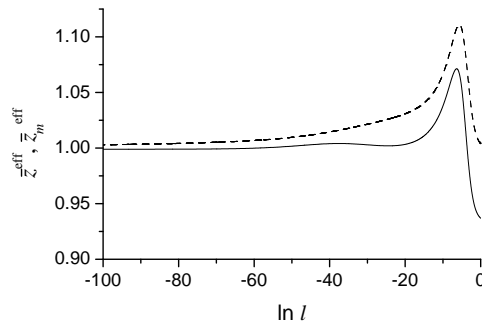


Figure 6. Dependencies of normalized effective dynamical critical exponents of the order parameter and conserved density correspondent to flow 4. Notations as if Fig. 5.

exponents occurs in different way for different flows, that means for different initial conditions. For system with small degree of disorder (small $u(0)$ and $w(0)$, flow 4) the approach of order parameter dynamical exponent to asymptotic regime is faster than for the conserved density one, while for system with larger amount of disorder (flow 2) approach of both quantities is almost simultaneous.

5. Conclusion

In this paper, we have studied model C dynamics of the random anisotropy magnets with cubic distribution of local anisotropy axis. For this purpose two-loop dynamical RG function ζ_Γ has been obtained. On the base of static results [3] the dependencies of effective critical exponents of order parameter, z^{eff} , and conserved density, z_m^{eff} , on the flow parameter were calculated.

The two-loop approximation adopted in our paper may be considered as certain compromise between what is feasible in static calculations from one side, and in dynamic ones from the other side. As a matter of fact, the state-of-the-art expansions of the static RG functions in the minimal subtraction scheme are currently available for many models within the five-loop accuracy [9, 44] but it is not the case for the dynamic functions. Complexity of dynamical calculations is reflected in the current situation, when the results beyond two loops have been obtained for model A only. The model C even with no structural disorder seems to be outside present manageable problems (see the recent review [5]). However, there are examples which demonstrate the even in two loops highly accurate results for dynamical characteristics can be obtained. One of them is given by the critical dynamics of ^4He at the superfluid phase transition [45]. Besides, analysis of the two-loop static RG functions refined by resummation also brings about sufficiently accurate quantitative characteristics of a static critical behavior in disordered systems [9, 46].

In the asymptotics the conserved density is decoupled from the order parameter and the dynamical critical behavior of random anisotropy model with cubic random axis distribution is the same as that of the random-site Ising model. Crossover occurring

between different FPs present in the random anisotropy model considerably influences the non-asymptotic critical properties. Different scenarios of dynamical critical behavior are observed depending of the initial values of the model parameters. The main feature is the presence of additional peaks on the curves for the effective dynamical critical exponents in comparison with the effective model A critical dynamics.

As far as the approach to the asymptotics is very slow, the effective exponents may be observed in experiments and in numerical simulations. The effective exponent for the order parameter may take a value far away from the asymptotic one (the asymptotic value in our two loop calculation is $z = 2.139$). The same holds for the conserved density effective critical exponent which may be far of its van Hove asymptotic value $z_m = 2$. For example one can observe values of z^{eff} and z_m^{eff} close to those for pure Ising model with model C dynamics.

This work was supported by Fonds zur Förderung der wissenschaftlichen Forschung under Project No. P16574

Appendix A. Perturbation expansion

We perform our calculations on the basis of the Lagrangian defined by (12) using the Feynman graph technique. The propagators for this Lagrangian are shown in the Fig. A1.

$$\begin{array}{ll}
 \begin{array}{c} k, \omega \\ i \end{array} \text{---} \begin{array}{c} k', \omega' \\ j \end{array} & G(k, \omega) \delta(k+k') \delta(\omega+\omega') \delta_{i,j} & \begin{array}{c} k, \omega \\ i \end{array} \text{---} \begin{array}{c} k', \omega' \\ j \end{array} & H(k, \omega) \delta(k+k') \delta(\omega+\omega') \delta_{i,j} \\
 \begin{array}{c} k, \omega \\ i \end{array} \text{---} \begin{array}{c} k', \omega' \\ j \end{array} & C(k, \omega) \delta(k+k') \delta(\omega+\omega') \delta_{i,j} & \begin{array}{c} k, \omega \\ i \end{array} \text{---} \begin{array}{c} k', \omega' \\ j \end{array} & D(k, \omega) \delta(k+k') \delta(\omega+\omega') \delta_{i,j}
 \end{array}$$

Figure A1. Propagators for constructing Feynman graphs. $G(k, \omega)$ and $H(k, \omega)$ are response propagators while $C(k, \omega)$ and $D(k, \omega)$ are correlation propagators.

Response propagators $G(k, \omega)$ and $H(k, \omega)$ are equal to

$$G(k, \omega) = 1/(-i\omega + \mathring{\Gamma}(\mathring{\mu} + k^2)) \quad \text{and} \quad H(k, \omega) = 1/(-i\omega + \mathring{\lambda}k^2), \quad (\text{A.1})$$

while the correlation propagators $C(k, \omega)$ and $D(k, \omega)$ are equal to

$$C(k, \omega) = 2\mathring{\Gamma}/|-i\omega + \mathring{\Gamma}(\mathring{\mu} + k^2)|^2 \quad \text{and} \quad D(k, \omega) = 2\mathring{\lambda}k^2/|-i\omega + \mathring{\lambda}k^2|^2. \quad (\text{A.2})$$

The vertices defined by Lagrangian are shown in Fig. A2.

We obtain an expression for the two-point vertex function $\mathring{\Gamma}_{\varphi\varphi}^{i,j}$ by keeping the diagrams up to two-loop order. The result of calculations can be expressed in form:

$$\mathring{\Gamma}_{\varphi\varphi}(\xi, k, \omega) = -i\omega \mathring{\Omega}_{\varphi\varphi}(\xi, k, \omega) + \mathring{\Gamma}_{\varphi\varphi}^{st}(\xi, k) \mathring{\Gamma}. \quad (\text{A.3})$$

Here we introduce the correlation length $\xi(\mathring{\mu} = \mathring{\mu} + \mathring{\gamma}\mathring{h}, \mathring{u}, \mathring{v}, \mathring{w}, \mathring{y})$, which is defined by

$$\xi^2 = \left. \frac{\partial \ln \mathring{\Gamma}_{\varphi\varphi}^{st}}{\partial k^2} \right|_{k^2=0}. \quad (\text{A.4})$$

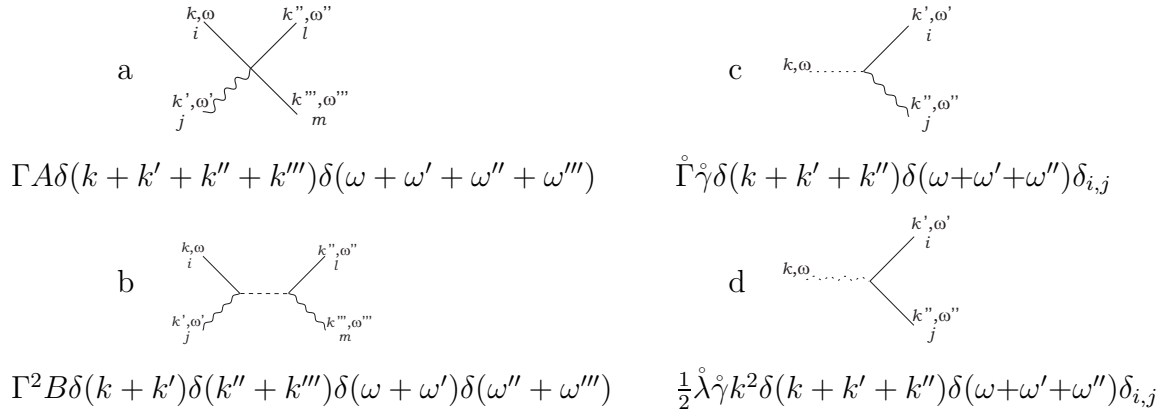


Figure A2. Vertices for our model. In vertex **a**, A stands for $v_0/3! (\delta_{i,j} \delta_{l,m} + \delta_{i,l} \delta_{j,m} + \delta_{i,m} \delta_{j,l})/3$ or $y_0/3! \delta_{i,j} \delta_{j,l} \delta_{l,m}$. In vertex **b**, B stands for $u_0/3! \delta_{i,j} \delta_{l,m}$ or $w_0/3! \delta_{i,j} \delta_{j,l} \delta_{l,m}$. Vertices **c** and **d** originate from the coupling to the conserved density.

The function $\overset{\circ}{\Gamma}_{\varphi\varphi}$ is the static two-loop vertex function of the disordered magnet. The structure (A.3) of the dynamic vertex function of pure model C was obtained in Ref. [43] up to two-loop order.

We can express two-loop dynamical function $\overset{\circ}{\Omega}_{\varphi\varphi}$ in the following form:

$$\overset{\circ}{\Omega}_{\varphi\varphi}(\xi, k, \omega) = 1 + \overset{\circ}{\Omega}_{\varphi\varphi}^1(\xi, k, \omega) + \overset{\circ}{\Omega}_{\varphi\varphi}^2(\xi, k, \omega), \quad (\text{A.5})$$

where the one loop contribution reads:

$$\overset{\circ}{\Omega}_{\varphi\varphi}^1(\xi, k, \omega) = -\frac{\dot{u} + \dot{w}}{3} \overset{\circ}{\Gamma} \int_{k'} \frac{1}{(-i\omega + \overset{\circ}{\Gamma}(\xi^{-2} + k'^2))(\xi^{-2} + k'^2)} + \gamma \overset{\circ}{\Gamma} I_C(\xi, k, \omega) \quad (\text{A.6})$$

while the two-loop contribution is of the form:

$$\begin{aligned} \overset{\circ}{\Omega}_{\varphi\varphi}^2(\xi, k, \omega) = & \overset{\circ}{\Gamma} \left(\frac{n+2}{18} \dot{v}^2 + \frac{\dot{y}^2}{6} + \frac{\dot{v}\dot{y}}{3} \right) \overset{\circ}{W}_{\varphi\varphi}^{(A)}(\xi, k, \omega) - \\ & \overset{\circ}{\Gamma} \left(\frac{n+2}{3} \dot{v} + \dot{y} \right) \dot{\gamma}^2 \overset{\circ}{C}_{\varphi\varphi}^{(T3)}(\xi, k, \omega) + \overset{\circ}{\Gamma} \dot{\gamma}^4 \overset{\circ}{S}_{\varphi\varphi}(\xi, k, \omega) + \\ & \overset{\circ}{\Gamma} \left(\frac{n+2}{9} \dot{v}\dot{u} + \frac{\dot{y}\dot{w}}{3} + \frac{\dot{w}\dot{v}}{3} + \frac{\dot{y}\dot{u}}{3} \right) \overset{\circ}{W}_{\varphi\varphi}^{(CD2)}(\xi, k, \omega) + \overset{\circ}{\Gamma} \left(\frac{\dot{u}^2}{9} + \frac{\dot{w}^2}{9} + 2\frac{\dot{w}\dot{u}}{9} \right) \times \\ & \left(\overset{\circ}{W}_{\varphi\varphi}^{(CD3)}(\xi, k, \omega) + \overset{\circ}{W}_{\varphi\varphi}^{(CD4)}(\xi, k, \omega) \right) - \\ & \overset{\circ}{\Gamma} \left(\frac{\dot{u} + \dot{w}}{3} \right) \dot{\gamma}^2 \left(\overset{\circ}{W}_{\varphi\varphi}^{(CD5)}(\xi, k, \omega) + \overset{\circ}{W}_{\varphi\varphi}^{(CD6)}(\xi, k, \omega) + 2\overset{\circ}{W}_{\varphi\varphi}^{(CD7)}(\xi, k, \omega) \right) \quad (\text{A.7}) \end{aligned}$$

In (A.6) and (A.7) the expressions for the integrals I_C , $\overset{\circ}{W}^{(A)}$, $\overset{\circ}{C}^{(T3)}$ and $\overset{\circ}{S}$ of the pure model C are given in the Appendix A.1 in Ref. [22], while the contributions for $\overset{\circ}{W}^{(CDi)}$ are presented in the Appendix of Ref. [13].

Following the renormalization procedure for $\overset{\circ}{\Gamma}_{\varphi\varphi}$ we obtain the two-loop renormalizing factor Z_{φ} :

$$Z_{\varphi} = 1 + \frac{2u + w}{\varepsilon} \frac{1}{3} - 2 \frac{\gamma^2}{\varepsilon} \frac{W}{1+W} + \frac{1}{\varepsilon^2} \left[\left(\gamma^2 \frac{W}{1+W} \left(\frac{1}{1+W} - \left(\frac{n}{2} - 1 \right) \right) - \right. \right.$$

$$\begin{aligned}
 & \left(\frac{n+2}{3}v + y \right) \gamma^2 \frac{W}{1+W} - \left(5 + \frac{W}{1+W} \right) \frac{u+w}{3} \gamma^2 \frac{W}{1+W} + \frac{2}{3}u^2 + \\
 & \frac{4}{3}uw + \frac{2}{3}w^2 + \frac{n+2}{9}uv + \frac{yu}{3} + \frac{vw}{3} + \frac{yw}{3} \Big] + \\
 & \frac{1}{2\varepsilon} \left\{ \left[\left(\frac{n+2}{3}v + y \right) \left(1 - 3 \ln \frac{4}{3} \right) + \gamma^2 \frac{W}{1+W} \left(\frac{n}{2} - \frac{W}{1+W} - \frac{3(n+2)}{2} \ln \frac{4}{3} - \right. \right. \right. \\
 & \left. \left. \left. \frac{1+2W}{1+W} \ln \frac{(1+W)^2}{1+2W} \right) \right] \gamma^2 \frac{W}{1+W} - \frac{11}{36}u^2 - \frac{3(n+2)}{36}uv - \frac{11}{18}uw - \frac{uy}{4} - \right. \\
 & \left. \frac{1}{4}vw - (u+w) \gamma^2 \frac{W}{1+W} \right\} - \frac{1}{\varepsilon} \left(\frac{n+2}{12}v^2 + \frac{vy}{6} + \frac{y^2}{4} \right) \left(\ln \frac{4}{3} - \frac{1}{12} \right) - \\
 & \frac{1}{\varepsilon} \frac{u+w}{3} \gamma^2 \frac{W}{1+W} \left[\frac{W}{2} \ln \frac{W}{1+W} - \frac{3}{2} \ln(1+W) - \frac{1}{2} \frac{W}{1+W} \ln W \right]. \quad (\text{A.8})
 \end{aligned}$$

- [1] R. Harris, M. Plischke, and M. J. Zuckermann, Phys. Rev. Lett. **31**, 160 (1973).
- [2] R. W. Cochrane, R. Harris, and M. J. Zuckermann, Phys. Reports, **48**, 1 (1978).
- [3] M. Dudka, R. Folk, and Yu. Holovatch, J. Magn. Magn. Mater., **294**, 305 (2005).
- [4] B. I. Halperin and P. C. Hohenberg, Rev. Mod. Phys. **49**, 436 (1977).
- [5] R. Folk and G. Moser, J. Phys. A: Math. Gen. **39**, R207 (2006).
- [6] As shown in: R.A. Pelcovits, E. Pytte, and J. Rudnick, Phys. Rev. Lett., **40**, 476 (1978); S.-k. Ma and J. Rudnick, Phys. Rev. Lett., **40**, 589 (1978), an absence of the ferromagnetic ordering for an isotropic random axis distribution at $d \leq 4$ follows from the Imry-Ma arguments first formulated in the context of the random field Ising model in: Y. Imry and S.-k. Ma, Phys. Rev. Lett. **35**, 1399 (1975). Later this fact has been proven by several other methods (see Ref. [3] for a more detailed account).
- [7] D. Mukamel and G. Grinstein, Phys. Rev. B **25**, 381 (1982).
- [8] M. Dudka, R. Folk, and Yu. Holovatch, in: W. Janke, A. Pelster, H.-J. Schmidt and M. Bachmann (Eds.), *Fluctuating Paths and Fields*, Singapore, World Scientific, 2001, p. 457; M. Dudka, R. Folk, and Yu. Holovatch, Condens. Matter Phys. **4**, 459 (2001).
- [9] For the recent reviews see e.g.: R. Folk, Yu. Holovatch, and T. Yavors'kii, Phys. Rev. B **61**, 15114 (2000); R. Folk, Yu. Holovatch, and T. Yavors'kii, Physics - Uspekhi **46** 169 (2003) [Uspekhi Fizicheskikh Nauk **173**, 175 (2003)]; A. Pelissetto and E. Vicari, Phys. Rep. **368**, 549 (2002).
- [10] U. Krey, Phys. Lett. A **57**, 215 (1976).
- [11] I. D. Lawrie and V. V. Prudnikov, J. Phys. C **17**, 1655 (1984).
- [12] M. Dudka, R. Folk, Yu. Holovatch, and G. Moser, Phys. Rev. E **72** 036107 (2005).
- [13] M. Dudka, R. Folk, Yu. Holovatch, and G. Moser, J. Phys. A **39** 7943 (2006).
- [14] B. I. Halperin, P. C. Hohenberg, and S.-k. Ma, Phys. Rev. B **10**, 139 (1974).
- [15] V. I. Corentsveig, P. Fraztl, and J. L. Lebowitz, Phys. Rev. B **55** 2912 (1997).
- [16] K. Binder, W. Kinzel, and D. P. Landau, Surf. Sci. **117** 232 (1982).
- [17] H. Tanaka, J. Phys.:Condens. Matter **11** L159 (1999).
- [18] G. Grinstein, S.-k. Ma, and G. F. Mazenko, Phys. Rev. B **15** 258 (1977).
- [19] P. Sen, S. Dasgupta, and D. Stauffer, Eur. Phys. J. B **1** 107 (1998).
- [20] D. Stauffer, Int. J. Mod. Phys. C **8** 1263 (1997)
- [21] R. Folk and G. Moser, Phys. Rev. Lett. **91**, 030601 (2003).
- [22] R. Folk and G. Moser, Phys. Rev. E **69** 036101 (2004).
- [23] E. Brezin and C. De Dominicis, Phys. Rev. B **12** 4954 (1975).
- [24] V.V. Prudnikov and A. N. Vakilov, Sov. Phys. JETP **74**, 900 (1992).
- [25] K. Oerding and H. K. Janssen, J. Phys. A: Math. Gen. **28**, 4271 (1995).
- [26] H. K. Janssen, K. Oerding, and E. Sengerspeick, J. Phys. A: Math. Gen. **28**, 6073 (1995).
- [27] V. Blavats'ka, M. Dudka, R. Folk, and Yu. Holovatch, Phys. Rev. B, **72** 064417 (2005)
- [28] A. B. Harris, J. Phys. C: Solid State Phys. **7**, 1671 (1974).

- [29] A. Aharony, Phys. Rev. B **12** 1038 (1975).
- [30] M. Dudka, R. Folk, and Yu. Holovatch, Condens. Matter Phys., **4**, 77 (2001); Yu. Holovatch, V. Blavats'ka, M. Dudka, C. von Ferber, R. Folk, and T. Yavors'kii, Int. J. Mod. Phys. B **16**, 4027 (2002).
- [31] P. Calabrese, A. Pelissetto, and E. Vicari, Phys. Rev. E **70**, 036104 (2004).
- [32] S.-k. Ma and J. Rudnick, Phys. Rev. Lett. **40**, 587 (1978).
- [33] C. De Dominicis, Phys. Rev. B **18**, 4913 (1978).
- [34] U. Krey, Z. Phys. B **26**, 355 (1977).
- [35] M. Dudka, R. Folk, Yu. Holovatch, and G. Moser, Condens. Matter Phys. **8**, 737 (2005)
- [36] R. Bausch, H. K. Janssen, and H. Wagner, Z. Phys. B **24**, 113 (1976).
- [37] V. J. Emery, Phys. Rev. B **11**, 239 (1975).
- [38] K. G. Wilson and M. E. Fisher, Phys. Rev. Lett. **28**, 240 (1972).
- [39] R. Schloms and V. Dohm, Europhys. Lett. **3**, 413 (1987); R. Schloms and V. Dohm, Nucl. Phys. B **328**, 639 (1989).
- [40] G. A. Baker, Jr., B. G. Nickel, and D. I. Meiron, Phys. Rev. B **17**, 1365 (1978).
- [41] P. J. S. Watson, J. Phys. A **7**, L167 (1974).
- [42] G. A. Baker, Jr. and P. Graves-Morris, *Padé Approximants* (Addison-Wesley: Reading, MA, 1981).
- [43] R. Folk and G. Moser, Acta Physica Slovaca **52**, 285 (2002).
- [44] H. Kleinert, J. Neu, V. Schulte-Frohlinde, K. G. Chetyrkin, and S. A. Larin, Phys. Lett. B **272**, 39 (1991); Erratum: Phys. Lett. B **319**, 545 (1993); H. Kleinert and V. Schulte-Frohlinde, Phys. Lett. B **342**, 284 (1995).
- [45] V. Dohm, Phys. Rev. B **44**, 2697; (1991), Phys. Rev. B **73**, 09990(E) (2006)
- [46] J. Jug, Phys. Rev. B **27**, 609 (1983).